#1500

# Design, Fabrication, and Application of a Dynamic Chamber for Measuring Gas Emissions from Soil

Fang Gao, S. R. Yates, M. V. Yates, Jianying Gan, and F. F. Ernst

Department of Soil and Environmental Sciences, University of California at Riverside, Riverside, California 92521, and USDA-ARS Salinity Laboratory, Riverside, California 92507

ENVIRONMENTAL® SCIENCE & TECHNOLOGY

Reprinted from
Volume 31, Number 1, Pages 148-153

*Environ. Sci. Technol. 1997. 37, 148-153*

# Design, Fabrication, and Application of a Dynamic Chamber for Measuring Gas Emissions from Soil

FANG GAO,*,† S. R. YATES,*
M. V. YATES,+ JIANYING GAN,‡ AND
F. F. ERNST+

***Department of Soil and Environmental Sciences, University of California at Riverside, Riverside, California 92521, and USDA-ARS Salinity Laboratory, Riverside, California 92507***

Dynamic or flow-through flux chambers are convenient tools for field measurements of gas fluxes from soils to the atmosphere. In this study, a dynamic flux chamber is designed and fabricated on the basis of aerodynamic considerations so that the conditions assumed for the flux model are closely satisfied. The chamber consists of an inlet transition zone, a square main body, and an outlet transition zone. Six equally-spaced air channels are installed in both inlet and outlet transition zones to conduct and spread the flowing air uniformly across the soil surface, which help to produce a simple, horizontal, and uniform airstream above the covered soil surface. Aerodynamic tests in the laboratory show that the air sweeps over the entire covered soil surface with a relatively constant velocity at a given air flow rate, and no stagnant air zones are present. The chamber is used in a field fumigation experiment to measure methyl bromide emission at the soil surface. The emission results obtained from the chamber are consistent with those obtained from micrometeorological methods used in the same experiment.

## Introduction

Emissions of soil trace gases into the atmosphere have long been studied from agricultural, ecological, and environmental perspectives. In the last decade or so, emissions of volatile organic compounds (VOCs) from the subsurface sources into the atmosphere have become a serious concern because of their potential threat to the health of human beings and their adverse effects on the environment. Many investigators have demonstrated that volatilization from soil to the atmosphere is one of the major loss processes of VOCs residing below the soil surface (I-3). Accurate measurement of the emission of trace gases and VOCs from soils to the atmosphere is essential for studying the behavior of gas movement and its fate in the subsurface, for evaluating existing theories and models of trace gas and VOC emissions, for estimating masses of trace gases and VOCs emitted into the atmosphere, and thus, for assessing the effects of such emissions upon the environment. A variety of techniques have been developed and used for the measurement of gas fluxes at the soil surface. These include various micrometeorological methods (e.g., aerodynamic method, eddy correlation, mass balance method, and energy balance method) and enclosure-based methods that consist of passive (or closed) and active (or dynamic, flow-through) flux chambers. Reviews and comparisons of these techniques are available (4- 7).

Dynamic (or flow-through) flux chambers have been widely used as convenient tools for measuring gas emissions from soil to the atmosphere (4, 5). This method involves placing an open-bottom chamber over a small soil surface, introducing an air flow through the chamber from the inlet to the outlet, and measuring the target gas concentrations in the m-coming air and the out-going air. In general, a flow-through chamber can be analyzed using the principle of mass balance over a time span of dt, which yields

$$\int_t \bar{Q}_{out}(t)\bar{C}_{out}(t)\,dt - \int_t \bar{Q}_{in}(t)\bar{C}_{in}(t)\,dt = \int_x\int_y\int_t [J_{diff}(x,y,t) + J^a_{adv1}(x,y,t)C_s(x,y,t) - J^a_{adv2}(x,y,t)C_a(x,y,t)]\,dt\,dy\,dx \quad (1)$$

where $x$ and y are the horizontal coordinates (L) at the enclosed soil surface, $J_{diff}$ is the diffusive mass flux of the target gas (M $L^{-2}t^{-1}$) at the enclosed soil surface, $J^a_{adv1}$ and $J^a_{adv2}$ are advective volume air fluxes (L $t^{-1}$) from and into the **soil matrix,** respectively, $C_s$ and $C_a$ are the target gas concentrations (M $L^{-3}$) at the soil surface on the soil side and on the air side, respectively. The terms $C_{in}$ and $C_{out}$ in eq 1 are the spatial average or representative concentrations of the target gas (M $L^{-3}$) in the in-coming air at the inlet and in the out-going air at the outlet, respectively. The terms $Q_{out}$ and $Q_{in}$ are the flow rates of the in-coming air and the out-going air ($L^3t^{-1}$), respectively, which can be expressed as

$$\bar{Q}_{out}(t) = \int_{A_1} v_1(\vec{s}_1,t)\,d\vec{s} \qquad \bar{Q}_{in}(t) = \int_{A_2} v_2(\vec{s}_2,t)\,d\vec{s} \quad (2)$$

where $v_1$ and $v_2$ are the air velocities (L $t^{-1}$) distributed on the outlet cross-section $A_1$ ($L^2$) and the inlet cross-section $A_2$ ($L^2$), respectively, and $\vec{s}_1$ and $\vec{s}_2$ are the area vectors on $A_1$ and $A_2$, respectively. The advective air fluxes ($J^a_{adv1}$ and $J^a_{adv2}$) in eq 1 can be caused by the flowing air through the chamber and the local change of barometric pressure within the chamber. For example, when the air flow has a local upward (or downward) component, a local $J^a_{adv1}$ (or $J^a_{adv2}$) will be induced. The terms $J^a_{adv1}C_s$ and $J^a_{adv2}C_a$ in eq 1 represent an upward and a downward advective mass flux of the target gas at the enclosed soil surface. The integral in eq 1 is over the entire enclosed soil surface. Equation 1 cannot be used to calculate flux because sufficient spatial and temporal information is difficult, if not impossible, to obtain.

In practice, the following assumptions are usually made: (1) the chamber is operating under steady state, i.e., the rate of air flow through the chamber is constant and not a function of time, (2) the gas flux is uniform over the entire covered surface and relatively constant during the sampling interval of ($t_2 - t_1$), (3) the in-coming airstream and the out-going airstream are well-mixed, i.e., $C_{out}$ and $C_{in}$ are representative, and (4) the diffusive flux ($J_{diff}$) is dominant and the advective mass flow is negligible. Under these assumptions, eq 1 can be reduced to

$$J = \frac{Q}{A}(\bar{C}_{out} - \bar{C}_{in}) \quad (3)$$

where $J$ is the mass flux (M $L^{-2}t^{-1}$), Q is the constant flow rate of air through the chamber ($L^3t^{-1}$), and $A$ is the enclosed soil surface area ($L^2$). The previously defined $\bar{C}_{out}$ and $C_{in}$ in eq 3 are measured in a time interval ($t_2 - t_1$). Equation 3 is the

* Corresponding author phone: (909)369-4846; fax: (909)342-4964; e-mail address: fgao@ussl.ars.usda.gov.
† University of California.
‡ USDA-ARS Salinity Laboratory.



S0013-936X(96)00251-9 CCC: $14.00 © 1996 American Chemical Society

standard approach to calculate the flux of the target gas at the soil surface when using flow-through chambers (4, 8).

Dynamic chambers with various shapes and operational features have been reported in the literature (8-13). Advantages of using dynamic chambers include (1) the potential to maintain the conditions within the chamber nearly the same as those in the surrounding field, since the ambient air is continuously flowing through the chamber, and (2) the elimination of a significant concentration buildup of the target gas in the chamber, since the target gas emitted from the covered soil into the chamber is continuously carried away to the outside environment by a clean in-coming airstream. One major disadvantage associated with dynamic chambers is that the air flowing in the chamber may change the pressure gradient between the soil-gas phase and the chamber interior. Such a change in the pressure gradient may create an advective mass flow of the target gas, which may be different from that created by the surface winds outside the chamber. For example, when the air in the chamber flows relatively fast and the wind outside the chamber is relatively slow, the flowing air in the chamber may create a pressure deficit, which produces an additional mass flow from the soil into the chamber. This pressure deficit **may result** in an overestimate of the emission from the uncovered soil (4, 7). Another **potential** problem with a dynamic chamber is associated with its aerodynamic behavior or air-flow pattern (5). If the chamber's inlet and outlet are not designed and installed properly, the flowing air through the chamber may not sweep over the entire covered surface, leaving local stagnant air zones inside the chamber. In addition, the air flow may have vertical components (downward or upward) that will exert a direct positive or negative pressure upon the covered soil surface. Both stagnant zones and vertical air-flow components can cause a spatially variable surface flux, which does not satisfy the conditions in deriving eq 3, and may also make the analysis of chamber behavior very difficult, if not impossible.

In this paper, we introduce a dynamic chamber that is designed and fabricated to closely follow the assumptions used in the standard flux model for the flow-through chambers (eq 3). Some of the factors that we believe to be important for obtaining efficient chamber design and operation are discussed. Results from the laboratory tests on the aerodynamic behavior of the chamber are presented and discussed. Finally, an example is presented using this chamber to measure the methyl bromide ($CH_3Br$) emission in a recent field fumigation experiment.

## Experimental Section

**Important Aspects in Chamber Design.** The chamber design and the materials used for the chamber construction affect the chamber aerodynamic behavior or air-flow pattemwhich, in turn, determines whether the chamber can properly measure the gas flux of interest. Important aspects to consider when designing and fabricating a dynamic chamber that will follow eq 3 include the following:

(1) The air flow in the chamber should sweep over the entire enclosed soil surface, eliminating any stagnant air zones in the chamber. Stagnant zones inside the chamber may lead to local concentration buildup, which reduces the flux locally below these zones, thus, violating the assumption of a constant flux in obtaining eq 3.

(2) The openings of the chamber's air inlet and outlet should be large enough to minimize pressure change due to air introduction and to ensure a relatively uniform velocity of the airstream in the chamber at the desired air flow rate. Thus, the effect of differential pressure created by the flowing air on flux will be uniform over the entire covered soil surface. This is also to ensure that a uniform flux is present under the chamber.

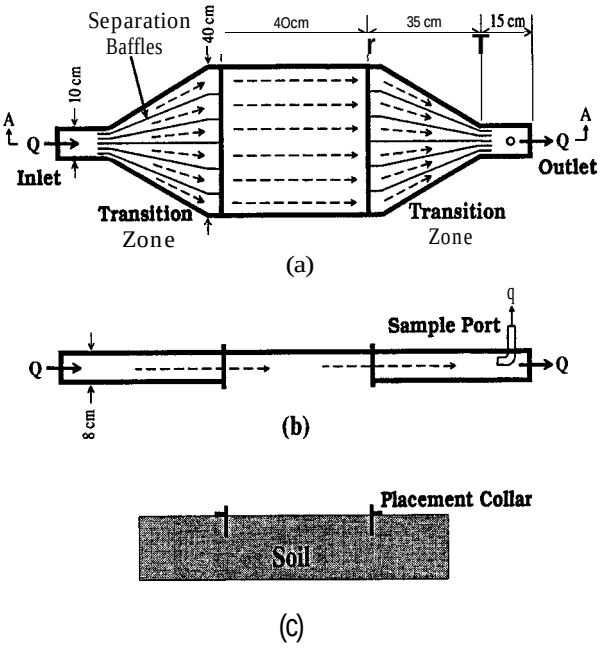


FIGURE 1. Schematic details of the flow-through chamber system: (a) top view, (b) cross-section A-A, and (c) base collar and soil matrix.

(3) The direction of the air flow in the chamber should be parallel to the covered soil surface, and any components of air flow perpendicular to the soil surface (either downward or upward) should be eliminated. Airstreams perpendicular to the enclosed soil surface may induce local advective mass flows from or into the soil matrix, which violates the assumption of a negligible mass flow for eq 3.

(4) The pattern of the air flow in the chamber should be relatively uniform across the swept soil surface to simplify the mathematical and physical representation and thus the analysis of such flow.

(5) Material for chamber fabrication should be strong and rigid to avoid possible structural deformation under field conditions. A deformed chamber body may cause leaks in the system and produce erroneous results.

(6) The outside surface of the chamber should be able to reflect solar radiation so that the radiant heating or the "greenhouse" effect can be effectively reduced. Our recent study has shown that this effect is important when the flow-through chambers are used on plastic tarp to measure methyl bromide fluxes (14).

Chamber Design and Fabrication. A dynamic chamber was designed using the criteria listed above. The schematic details of the chamber are shown in Figure 1. The chamber consists of (Figure 1a, from the left to the right): air inlet, inlet transition zone, chamber main **body** that covers the soil surface, outlet transition zone, sampling port, and air outlet. Within each transition zone, five baffles were designed to divide the transition zone into six individual equal-volume channels to spread the in-coming air evenly across the soil surface.

The desired air flow pattern in the dynamic chamber is shown in Figure 1 by the dashed-line arrows. When the air enters the inlet, it is split into six equally-spaced channels. At the ends of these channels, the six streams of air are expected to have the same velocity and to sweep horizontally across the soil surface toward the outlet transition zone. After sweeping over the enclosed soil surface, the flowing air is split again and then conducted by the six channels in the outlet transitionzone to the outlet. Gas samples can be taken from the airstream at the inlet and the outlet (sample port at the inlet is not shown).

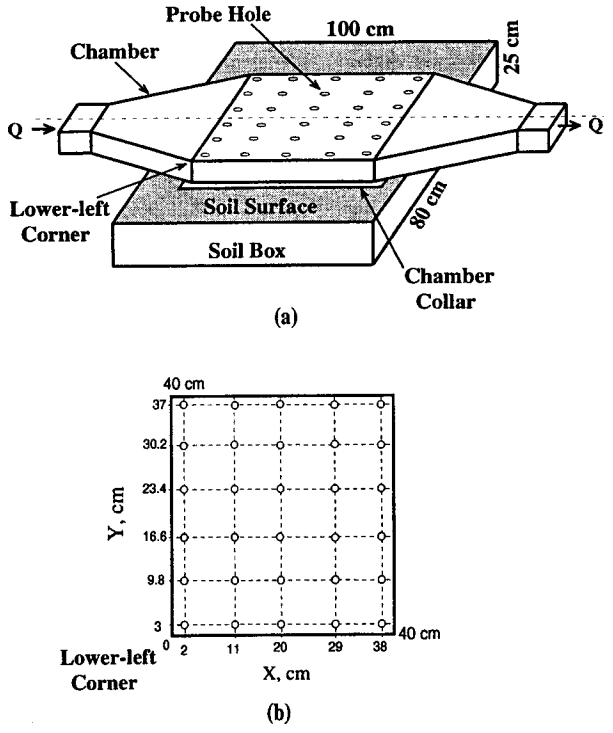


**FIGURE 2. Laboratory tests on chamber aerodynamic behavior: (a) experimental setup and (b) locations of probe holes.**

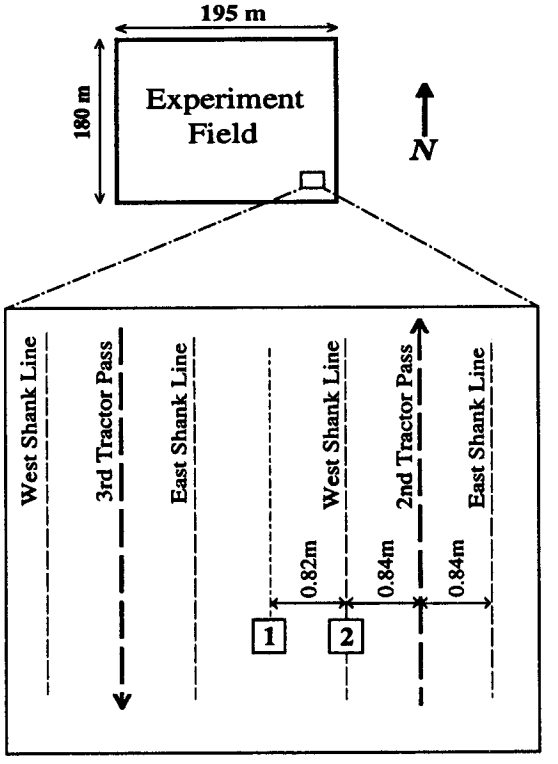


**FIGURE 3. Experiment field and chamber operation positions.**

For field application, a dynamic chamber was fabricated with the dimensions shown in Figure 1a. The entire chamber body was made with 20-gauge galvanized sheet metal. The air diverting baffles in the transition zones were made with 26-gauge galvanized sheet metal. To obtain the desired rigidity, the main body of the chamber, which covers the soil surface, had a skeleton made of 2.5 cm (1 in.) angle iron. The sampling port at the outlet was made of a brass tube with an i.d. of 1 cm and a length of 5 cm (Figure 1b). The top cover of the chamber is removable so that a transparent cover can be installed to facilitate tests on the aerodynamic behavior of the chamber in the laboratory. When operating in the field, the chamber sits on a base collar that was made of 20-gauge galvanized sheet metal and 2.5 cm (1 in.) angle aluminum as the guiding edge and sitting base (Figure 1c). The collar can be inserted into the soil to a depth of 10 cm to support the chamber at the soil surface. The air flow through the chamber system is achieved by applying a vacuum at the outlet side. The outside surface of the entire chamber is painted with white latex paint to reduce radiant heating.

**Laboratory Tests on Chamber Aerodynamic Behavior.** To study the aerodynamic behavior of our chamber and to evaluate whether the chamber could meet the design criteria, the chamber was tested in the laboratory to determine air velocity distribution within the chamber. The experimental setup is shown in Figure 2a. The exact dimensions of the chamber are $W$ (width) = 40.2 cm, $L$ (length) = 40.5 cm, and $H$ (height) = 9.5 cm, where the height of the chamber is the distance from the soil surface to the top cover. To allow measurement of the air velocity inside the chamber, a transparent PVC (polyvinyl chloride) cover, 0.6 cm (1/4 in.) thick, was installed, and 30 holes (0.5 cm in diameter) were evenly distributed on the cover (Figure 2b). The velocity of the flowing air inside the chamber was measured using a low-velocity (reported range of 0.5–50 cm $s^{-1}$) anemometer Model AVS4-08 (American Data Cable, Inc., Placerville, CA). This device has thin-wire sensors about 5 cm long that can be inserted into the chamber through the holes on the chamber cover. The chamber was operated by a laboratory vacuum system. When the air velocity was measured through one hole, all other holes were sealed with small rubber stoppers. The anemometer sensor was placed about 2 cm above and perpendicular to the soil surface. The air flow rate ($Q$) through the chamber was monitored by a Gilmont ball flowmeter (Gilmont Instruments, Inc., Barrington, IL). Three tests were conducted and the flow rates used were $Q_1 = 24.5$, $Q_2 = 49.5$, and $Q_3 = 74.5$ L $min^{-1}$, respectively.

**Application in Field Experiment.** During May 1994, the chamber was used in a field experiment to measure the methyl bromide emission from uncovered fumigated soil. A 3.5-ha (195 m × 180 m) field containing the Greenfield sandy loam (a coarse-loamy, mixed, thermic Typic Haploxeralf) was used in the experiment for the deep injection of the fumigant (Figure 3). During the first day of the experiment, methyl bromide was injected at a depth of approximately 68 cm (27 in.) below the soil surface through a set of tractor-mounted shanks, separated by 1.68 m (5.5 ft) and connected to steel cylinders containing pressurized methyl bromide liquid. The fumigation operation started shortly after 12:00 noon of the first day of the experiment. During the 4-h fumigation operation, approximately 1134 kg of methyl bromide was injected into the soil, and a total of 59 tractor passes down the field were run. Figure 3 shows the second and third tractor passes in the fumigation operation.

The dynamic chamber was positioned near the southeast corner of the field (Figure 3). Position 1 was located approximately midway between the second and the third tractor passes. Position 2 was approximately on the west shank line of the second tractor pass. One hour after the tractor finished the second pass, the chamber at position 1 was turned on and operated at this position for 2 h. The chamber was then moved to position 2 for the next 2-h interval. The chamber operation at one position (position 1 or 2) was kept for 2 h during the first 12 days of the experiment. Longer operation times (4, 6, and 10 h) at each position were used in the following 7 days of the experiment. The chamber was operated continuously for a period of 19 days.

The chamber air flow was driven by connecting a vacuum to the outlet side. At the inlet, the in-coming air was introduced through an aluminum pipe with an i.d. of 7.6 cm (3 in.). One end of this aluminum pipe was connected to the

chamber inlet, and another end was open to the air 10 cm above a nonfumigated field approximately 100 m (328 ft) south of the experiment site. Samples were taken at this nonfumigated site during the experiment. Calculation using Poiseuille's law showed that drawing air through the 100-m pipe may create a small pressure deficit in the chamber (approximately03 Pa). This pressure deficit was insignificant as compared to the ambient barometric pressure fluctuation, which was l-2 orders of magnitude greater as indicated by the barometric pressure data continuously recorded during the experiment (15). The chamber air flow rate (Q) was adjusted to 7.4 L $min^{-1}$ by an in-line control valve. With this flow rate, the air in the chamber was completely exchanged approximately every 2 min (i.e., the residence time), since the chamber main body had a volume of about 15 L. Temperatures within the chamber during the operation were f1.5 °C as compared to the ambient air temperatures outside the chamber.

Samples at the outlet were obtained from the sample port by passing a portion of the chamber out-going air through charcoal sampling tubes (Supelco Inc., Bellefonte, PA) at a flow rate of 0.1 L $min^{-1}$. The samplingflowrate was controlled by an in-line microvalve. This flow rate was monitored every 1 s using a turbine-wheel gas flow sensor (McMillan Co., Georgetown, TX), averaged over a 5-min interval **and recorded** by an on-site computer. During each sampling interval, i.e., while the chamber was operating at one position, the air withdrawn from the sample port passed through a series of three charcoal tubes (or two tubes in the last 5 days of the experiment). Each tube contained approximately 600 mg of activated coconut charcoal granules (20/40 mesh). At the end of each sampling interval, the charcoal tubes were removed, the chamber was moved to the next position, a new series of tubes were installed, and the chamber air flow rate was adjusted, **if necessary,** to 7.4 L $min^{-1}$. The removed tubes were capped at both ends and placed in a freezer at -4 °C for temporary storage of less than 12 h before being transported to the laboratory for analysis. For analysis, benzyl alcohol was used to extract the methyl bromide sorbed on charcoal granules. Analysis of the methyl bromide trapped on the charcoal granules was conducted with a computer-operated HP 5890 Series II gas chromatograph (Hewlett-Packard Co., Avondale, PA) and a Telonar 7000 headspace autosampler (Telonar Company, Cincinnati, OH). Details of the analytical procedure are given elsewhere (16).

## Results and Discussion

**Chamber Aerodyanmic Behavior.** The distributions of air velocity as a function of the volumetric flow rate within the dynamic chamber are shown in Figure 4a–c. The nominal velocity ($V_o$) *in* a test is calculated using $V_o = Q/(WH)$ where Q is the volumetric flow rate through the chamber, and *W* and *H are the* chamber width and height, respectively. The averaged velocity ($V_a$) is the arithmetic average of 30 velocities measured within the chamber at about 2 cm above the soil surface. Since the length of the velocity sensor is 5 cm, each measured velocity **represents** an average of the horizontal air velocity between 2 and 7 cm from the soil surface.

The results of three air velocity tests are summarized in Table 1. In Test 1, the 30 measured velocities are from 60% to 160% of the measured average and from 55% to 145% of the calculated nominal velocity. In test 2, the measured velocities are from 60% to 148% of the measured average and from 68% to 168% of the calculated nominal velocity. In test 3, the measured velocities are from 71% to 146% of the measured average and from 76% to 155% of the calculated nominal velocity.

When the results from these tests are plotted as perspective diagrams, they show clearly that there are no stagnant zones above the enclosed soil surface while the chamber is in operation (Figure 4a–c). The discrepancy between the

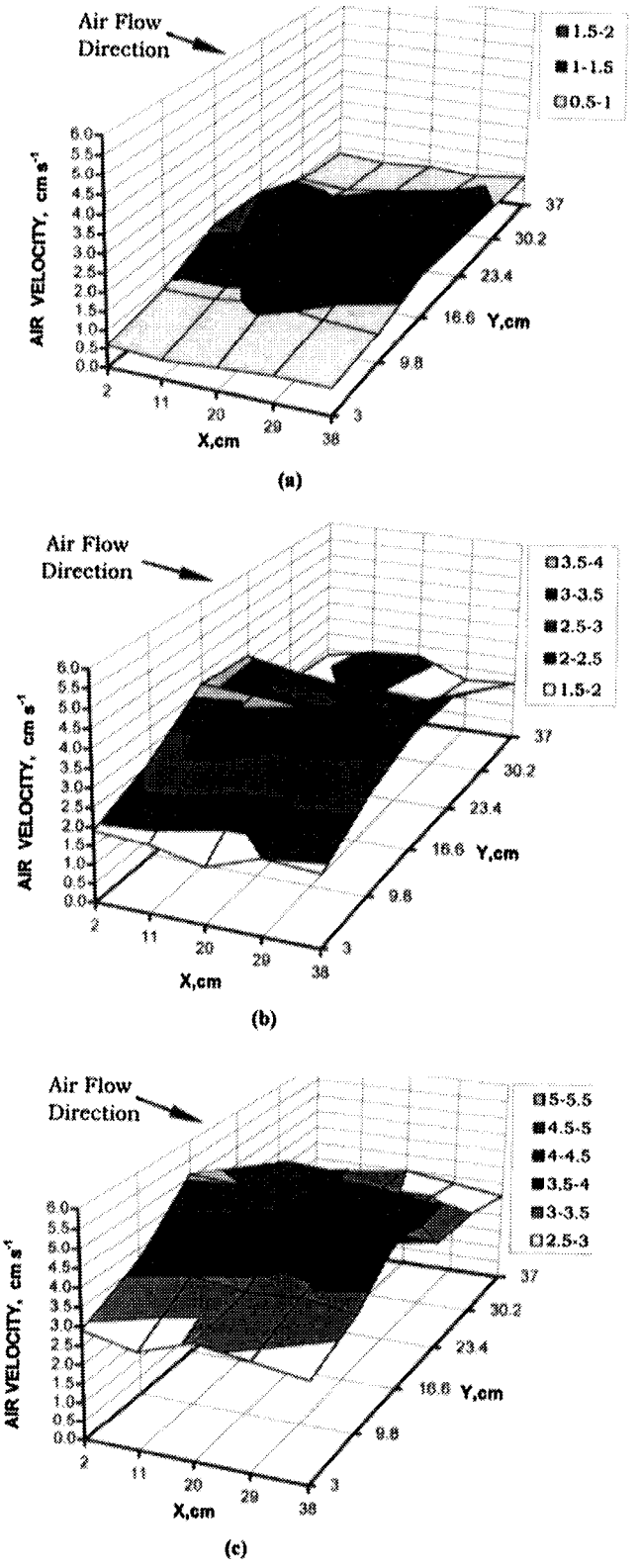


FIGURE 4. Distributions of the flowing air velocity in the chamber: (a) $Q_1$ = 24.5 L $min^{-1}$, (b) $Q_2$ = 49.5 L $min^{-1}$, (c) $Q_3$ = 74.5 L $min^{-1}$.

measured average velocities and the nominal velocities calculated from the **flow** rate (Q) and the chamber dimensions *(W and H)* are within ±15%. All three tests show a faster longitudinal airstream in the middle of the chamber (Figure 4a–c). This is likely due to the effect of chamber side walls and the central position of the vacuum source. This effect could be minimized or eliminated by adjusting the opening positions of the air diverting baffles at the inlet so that a slightly greater amount of air could be directed toward the

TABLE 1. Flowing Air Velocities in Dynamic Chamber

| test | air flow rate Q (L/min) | calculated velocity $v_0$ (cm/s) | measured velocities $v_a$ (cm/s) range | measured velocities $v_a$ (cm/s) average | $v_a/v_0$ ratio |
|---|---|---|---|---|---|
| 1 | 24.5 | 1.1 | 0.6-1.6 | 1.0 | 0.91 |
| 2 | 49.5 | 2.2 | 1.5-3.7 | 2.5 | 1.14 |
| 3 | 74.5 | 3.3 | 2.5-5.1 | 3.5 | 1.06 |

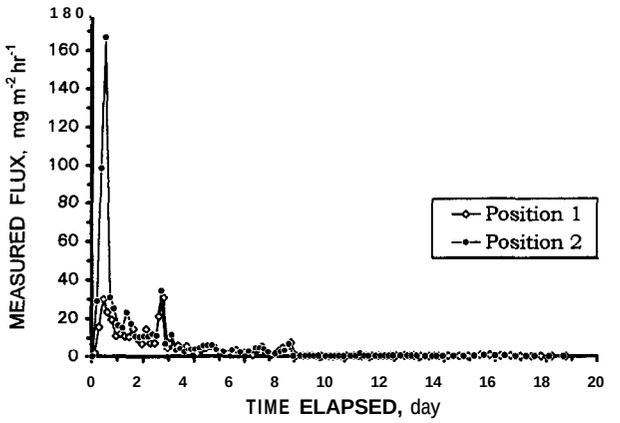


FIGURE 5. Methyl bromide fluxes measured in 19 days in the field experiment

outer edges of the chamber, thus increasing the air velocity in this region. The anemometer used in these tests is not able to determine the vertical air velocity in the chamber. Based on the structure of the chamber, it could be expected that there is no bulk vertical air flow in the chamber. In a preliminary test, a visible smoke tracer was used to view the air flow pattern inside the chamber. No vertical airstreams were observed in the chamber through the transparent cover.

Results from Field Application. Samples taken from the chamber in-coming air during the experiment showed-that the in-coming air was free of the target fumigant (i.e., $C_{in}$ = 0). Since charcoal tubes were used to collect the methyl bromide gas from the sampling port, eq3 is modified as follows to calculate methyl bromide flux:

$$J_i = \frac{Q + q_i}{A} \frac{m_i}{q_i \Delta t_i} \quad (4)$$

where $J$ (mg $m^{-2}$ $h^{-1}$) is the flux density, Q (L $min^{-1}$) and q (L $min^{-1}$) are the out-going air flow rate and the sample port air flow rate, Q + q is the total air flow through the chamber (Figure lb), $A$ ($m^2$) is the enclosed surface area, $m$ (mg) is the chemical mass adsorbed by the charcoal tubes in an individual sampling event, and At (h) is the sampling time interval for the corresponding tube series. The subscript i represents an individual sampling event. The flux density ($J_i$) calculated by eq 4 is the flux averaged over the time interval of the sampling event *i*. The results of flux calculations are shown in Figure 5. On the time axis in Figure 5, a numbered position represents the noontime (i.e., 12:00 PM) of that day.

From Figure 5, it can be seen that the emission fluxes measured at position 2 were greater than those at position 1 in the first three days, and especially for the first day, of the experiment. Such differences in emissions were likely due to the disturbance of soil structure by the injection shanks during the fumigation operation. When pulled by the tractor, each shank created a narrow fracture to a depth of 68 cm. At the bottom of this fracture, methyl bromide was injected as a liquid and became a concentrated vapor immediately after injection. Although the fracture was pushed closed at the soil surface, the disturbed soil in the region of the fracture was likely more porous and included continuous pathways

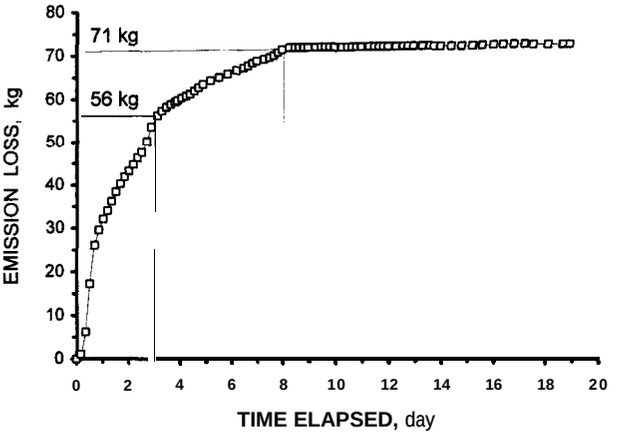


FIGURE 6. Cumulative emission loss of methyl bromide in 19 days in the field experiment.

as compared to the original soil matrix. These loosely-filled fractures could **allow** methyl bromide to migrate much faster, especially during the early stage of the experiment when the fumigant vapor concentration was very high in the near vicinity of the source lines (i.e., the bottoms of the fractures). This **explanation** is qualitatively in agreement with the results of a simulation study of dense vapor migration in fractured geologic media reported by Shikaze et al. (17). After 1 day or so, the concentration of methyl bromide in the vicinity of the source lines dropped due to the rapid mass loss through the fractures, and the effect of the vapor pressure on methyl bromide migration became less significant. As the fumigant became more evenly distributed in the horizontal direction, the differences in emissions at position 1 and position 2 became less noticeable, as shown in Figure 5.

To calculate the total emission of methyl bromide, the average of the flux density measured at position 1 and the flux at position 2 is used. The cumulated emission of methyl bromide over the entire experimental field as a function of time is shown in Figure 6. On the time axis in Figure 6, a numbered position represents the noontime (i.e., 12:00 PM) of that day. Figure 6 shows that the emission of methyl bromide in the first three days accounted for more than 75% of the total emitted mass, while more than 95% of the total emitted mass occurred in the first 8 days. These results are in agreement with the results from some recent field experiments, which also show that the major portion of the volatilization loss of methyl bromide from fumigated fields is due to the early days' emissions (18-20). The total emission loss from the entire field in our experiment is estimated to be 72.4 kg, which was about 6.4% of the total fumigant applied to the field. For our experiment and its field conditions, this percentage of mass loss due to the volatilization as estimated by the chamber measurements is in agreement with the emission results measured by the aerodynamic methods in the same experiment, which show a range of total emission between 3 and 5% (S. R. Yates, 1994, unpublished data).

The design and structure of the dynamic chamber presented in this paper may provide further research opportunities. First, it allows the analysis of chamber behavior by developing physical and mathematical models since the chamber produces a simple, horizontal, and uniform airstream. Second, a chamber with a similar structure can be used to simulate horizontal surface wind that sweeps over a small land surface where gas emission occurs. Thus, effects of horizontal surface wind on emission can be simulated and studied. Third, if the chamber operates in connection with an anemometer, which measures the external wind speed, this information can be used as a control to regulate the chamber flow rate, and synchronization between surface wind outside the chamber and the airstream inside the chamber

**can be accomplished. Thus, a more accurate measurement of the flux in the field will become possible with this chamber.**

## Acknowledgments

**This study was supported by USDA Cooperative State Research Service** Agreement **92-34050-8152. Thanks are due to A. Mutziger, P. Pacheco, and D. Wang for their help in obtaining the field experimental data reported herein.**

## literature Cited

(1) Jury, W. A.; **Spencer, W. F.; Fanner, W.** J. ***J. Environ. Qual.*** 1983, 12, 558-564.

(2) Glotfelty, D. E.; Taylor, A. W.; Turner, B. C.; Zoller, W. H. ***J. Agric. Food Chem.*** 1995, 32, 638-643.

(3) Taylor, A. W.; Spencer, W. F. In ***Pesticides in the Soil Environment;*** Cheng, H. H., Ed.; Book Series No. 2; Soil Science Society of America: Madison, WI. 1990; DD 213-269.

(4) Rolston, D. E. In ***Methods of Soil Analysis. Part 1. Physical and Mineralogical Methods,*** 2nd ed.; Klute, A., Ed.; American Society of Agronomy Madison, WI, 1986; pp 1103-1119.

(5) Wesely, M. L.; Lenschow, D. H.; Denmead, 0. T. In Global ***Trovosvheric Chemistry: Chemical Fluxes in the Global Atmosphere***; Lenschow, D. H., Jicks, B. B., Eds.; National Center for Atmospheric Research: Boulder, CO, 1989; pp 31-46.

(6) Majewski, M. S.; Glotfelty, D. E.; U, K. T. P.; Seiber, J. N. ***Environ. Sci. Technol.*** 1990,24, 1490-1497.

(7) Denmead, 0. T.; Raupach, M. R. ***In Agricultural Ecosystem Effects on Trace Gases and Global Climate Change;*** Special Publication No. 55; Soil Science Society of America: Madison, WI, 1993; pp 19-43.

(8) Denmead, 0. T. ***Soil Sci. Soc. Am. J. 1979, 43, 89-95.***

(9) Schmidt, C. E.; Balfour, W. D. In ***Proceedings of the 1983 ASCE National Specialty Conference on Environmental Engineering; American Society*** of Civil Engineers: New York, 1983; pp 690-699.

(10) Sanders, P. F.; McChesney, M. M.; Seiber, J. N. ***Bull. Environ. Contam. Toxicl.*** 1985, 35, 569-575.

(11) Clendening, L. D. A field mass balance study of pesticide volatilization, leaching **and** persistence. Ph.D. Thesis, University of California, Riverside, CA, 1988.

(12) Morrison, M. C.; Hines, M. E. Atmos. ***Environ.*** 1990, 24, 1171-1179.

***(13)*** Valente, R. J.; Thornton, F. C.; Williams, E. J. ***J. Geophys. Res.*** 1995, ***100,*** 21,147-21,152.

***(14)*** Yates, S. R.; Gan, J.; Ernst, F. F.; Wang, D. ***J. Environ. Qual. 1988, 2.5, 892-898.***

***(15)*** Yates, S. R.; Gan, J.; Ernst, F. F.; Mutziger, A.; Yates, M. V. ***J. Environ. Qual.*** 1998, ***25,*** 184-192.

***(16)*** Gan, J.; Yates, S. R.; Spencer, W. F.; Yates, M. V. ***J. Agric. Food Chem.*** 1995, 43, 960-966.

***(17)*** Shikaze, S. G.; Sudicky, E. A.; Mendoza, C. A. ***Water Resour. Res. 1884, 30,*** 1993-2009.

***(18)*** Yates, S. R.; Ernst, F. F.; Gan, J.; Gao, F.; Yates, M. V. ***J. Environ. Qual.*** 1996,25, 192-202.

***(19)*** Yagi, K.; Wiiiams, J.; Wang N.-Y.; Cicerone, R. J. ***Science*** 1995, ***267,*** 1979-1981.

***(20)*** Majewski, M. S.; McChesney, M. M.; Wooddrow, J. E.; Seiber, J. N.; Pruger, J. **Aerodynamic *Volatilization Measurements of Methyl Bromide from Tarped and Untarped Fields.*** Project Report, Center for Environmental Sciences and Engineering, University of Nevada: Reno, NV, 1994.

***Received for review March 18, 1996. Revised manuscript received August 14, 1996. Accepted August 14, 1996.***[⊗]

**ES9602511**

**@Abstract** published in *Advance ACS Abstracts,* November 1,1996.